SOLA, 2016, Vol. 12, 247−252, doi:10.2151/sola.2016-049

Supplemental material A:

Relationship between environmental parameters and forecast errors for TCs over land and coastal regions

We summarize the relationship between environmental parameters and forecast errors in coastal regions and over land. Here, the environmental parameters used are the vertical wind shear, CAPE, T_s, and E-MPI. Figures A1 and A2 show the mean biases of MSLP and Vmax with respect to these parameters for coastal regions and land, respectively. For coastal regions, the excessively intense TCs were predicted in RSMC Tokyo official forecasts when E-MPI expected relatively weak TCs compared to RSMC Tokyo forecast. Mean biases with respect to the vertical wind shear, CAPE and T_s were not clear. For landfalling TCs, the behavior of errors shows that recent official forecasts contain biases with respect to the vertical wind shear, CAPE, and E-MPI (Figs. 4 and 5). However, these features are not as clear as in the open ocean cases, possibly because the number of cases is small.

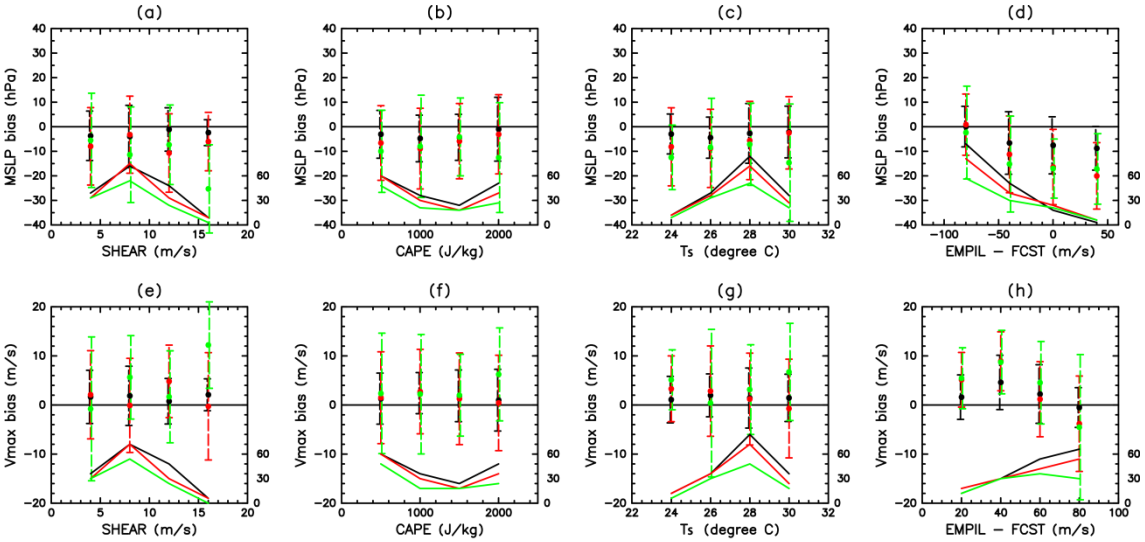

Fig. A1. Biases of the forecasts for TCs in the coastal region (a)-(d) MSLP forecasts and (e)-(h) Vmax forecasts related to physical environmental parameters: (a)(e) magnitude of vertical shear of horizontal wind, (b)(f) CAPE, (c)(g) T_s, and (d)(h) deviation in E-MPI relative to an intensity metric derived from RSMC Tokyo forecast.

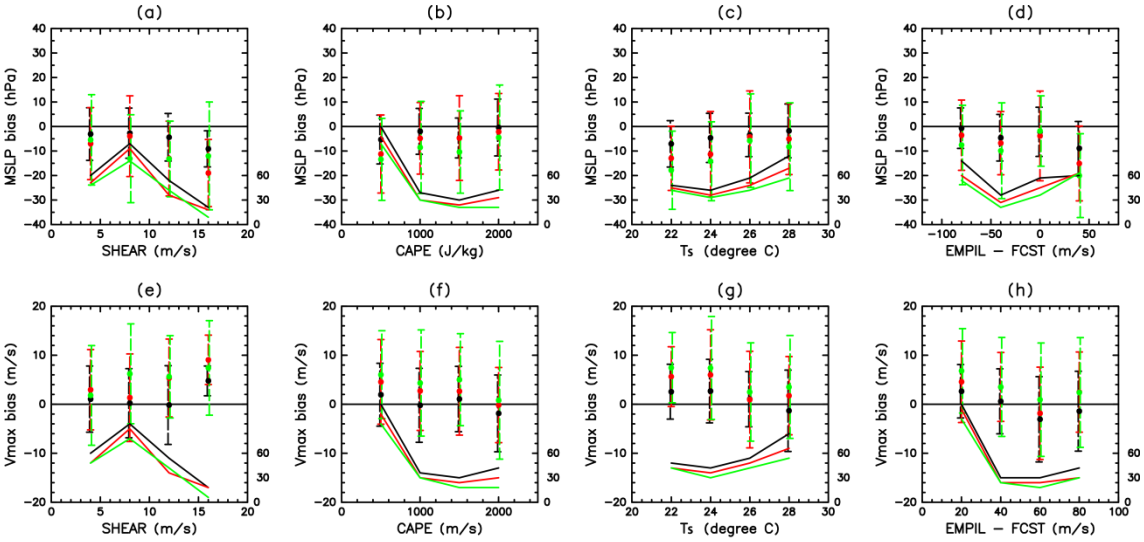

Fig. A2. Same as Fig. A1 but for landfalling TC forecasts.

Supplemental material B

Additional statistical correction experiments

a. The use of high-resolution oceanic reanalysis

In the main text, T_{100} was calculated from the 3D-Var-based parent domain output with coarse grid spacing of 0.5° by 0.5° prepared for the dataset of Four-dimensional Variational Ocean ReAnalysis for the WNP over 30 years (Usui et al. 2016, manuscript submitted to *J. Oceanogr.*). The 4D-Var-based high-resolution oceanic outputs with a grid spacing of 0.1° by 0.1° are not used in the main manuscript because this dataset (15°N–60°N and 118°E–180°E) does not cover the whole region which the RSMC Tokyo is responsible for in terms of analysis and prediction of TCs. However, one may wonder if the use of sophisticated oceanic dataset really enhances the accuracy of TC intensity forecasts. Therefore, we conducted another statistical correction experiment in which T_{100} is calculated using the fine-mesh domain output. For a fair comparison, care was taken to only include cases where T_{100} was available both in the parent domain and fine-mesh domain.

The use of fine-mesh output slightly reduces RMSEs of the official TC

intensity forecasts more than the use of parent domain output (Table B1). Improvement rates increase by about 1%. Although this difference between results obtained from parent domain and fine-mesh domain is not detected as significant change, it exhibits the potential of high-quality oceanic data for further improvements in the TC intensity forecasts.

b. Statistical correction applied to the JMA-GSM

In this subsection, the forecast skill of a statistically corrected GSM output is evaluated rather than the correction of the RSMC official forecasts. To do so, the following simple linear regression is considered:

$$G' = G + \alpha_1 S + \alpha_2 \mathrm{CAPE} + \alpha_3 \mathrm{MSLP\_PI} + \alpha_4 \mathrm{MSLP\_GSM} + \beta + \varepsilon$$

where G and G' represent the predicted TC intensity obtained from JMA-GSM and a statistically corrected forecast, respectively. The calculation procedure is the same as in the main text. This correction scheme does not consider TC intensity errors at the initial time of forecasts. TC intensity forecasts may thus suffer from adverse effects of initial TC intensity errors, particularly for intense TCs that are not reproduced properly by the JMA-GSM. Therefore, a different form of linear regression is also tested:

$$G'' = G + \alpha_1 S + \alpha_2 \mathrm{CAPE} + \alpha_3 \mathrm{MSLP\_PI} + \alpha_4 \mathrm{MSLP\_GSM} + \alpha_5 \left(G_{init} - B_{init} \right) + \beta + \varepsilon$$

where G_{init} and B_{init} represent the TC intensity metric (MSLP or Vmax) at the initial time of forecasts obtained from JMA-GSM and in the best track, respectively. Although a real time initial TC intensity analysis is more suitable as B_{init} for constructing a realistic guidance, we used the TC intensity best track because the real time TC intensity analysis was not available to us.

Table B2 shows RMSEs for the RSMC Tokyo official forecasts (F), G, G', and G''. Statistically corrected JMA-GSM-based forecasts for FT = 72 h over the open ocean are generally better than the RSMC Tokyo official forecasts, while TC intensity forecasts obtained from JMA-GSM are originally less accurate than the official forecasts. The JMA-GSM-based forecasts are more performant for TCs over land or coastal regions. The initial TC intensity error correction improved the accuracy of the JMA-GSM forecast at FT = 24 h, despite overall lower performances compared to the official forecasts. By comparing Table 1 with Table B2, it is found that the statistically corrected official forecasts outperform the statistically corrected JMA-GSM forecasts.

Table B1. RMSEs for *F* (RSMC Tokyo official forecasts), *L* (Corrected official forecasts based on the low-resolution oceanic dataset), and *H* (Corrected official forecasts based on the high-resolution oceanic dataset). Results are expressed as average ± standard deviation, over seven one-year groups.

Exp.	FT	RMSE (F)	RMSE (L)	RMSE (H)
MSLP (OC_PI)	24	13.6±0.8	12.2±1.0	12.1±1.0
	48	19.8±1.5	16.6±2.0	16.5±2.1
	72	21.8±2.4	18.2±2.7	18.1±2.7
Vmax (OC_PI)	24	6.1±0.6	5.6±0.8	5.5±0.7
	48	8.4±1.0	7.2±1.2	7.1±1.2
	72	9.1±0.7	7.7±1.2	7.6±1.2

Table B2. RMSEs for *F* (RSMC Tokyo official forecasts), *G* (JMA-GSM forecast), *G*' (first statistically corrected JMA-GSM forecast), and *G*"(second statistically corrected JMA-GSM forecast). Results are expressed as average ± standard deviation, over seven one-year groups. Improvement rates significantly lower (higher accuracy) than those obtained for *F* at the 95% confidence level are shown in bold, while degenerations (lower accuracy than F) are in italics.

Exp.	FT	RMSE (F)	RMSE (G)	RMSE (G')	RMSE (G")
MSLP (E-MPIO)	24	13.5±0.9	*23.6±3.2*	*18.9±1.7*	*14.8±1.0*
	48	20.0±1.8	*26.1±3.1*	20.5±1.7	20.3±1.5
	72	22.1±1.9	*26.9±3.2*	21.3±2.0	21.3±2.1
MSLP (OC_PI)	24	13.5±0.9	*23.6±3.2*	*17.8±1.7*	14.0±1.2
	48	20.0±1.8	*26.1±3.1*	**18.9±1.4**	**18.7±1.3**
	72	22.1±1.9	*26.9±3.2*	**19.6±1.4**	**19.6±1.4**
MSLP (E-MPIL)	24	10.5±1.9	11.2±2.4	10.5±2.2	9.5±1.8
	48	16.3±2.2	14.9±2.3	**12.1±2.8**	**12.1±2.9**
	72	20.6±1.6	**16.2±2.6**	**13.5±2.1**	**13.7±2.3**
Vmax (E_MPIO)	24	6.2±0.5	*11.5±1.4*	*8.0±1.0*	*6.9±0.7*
	48	7.8±1.0	*12.1±1.6*	8.6±1.2	8.6±1.2
	72	9.3±0.7	*12.0±1.4*	9.0±1.0	8.9±1.0
Vmax (OC_PI)	24	6.2±0.5	*11.5±1.4*	*7.6±1.1*	6.5±0.7
	48	7.8±1.0	*12.1±1.6*	8.1±1.3	8.1±1.3
	72	9.3±0.7	*12.0±1.4*	**8.5±1.2**	**8.5±1.2**
Vmax (E_MPIL)	24	6.4±1.2	6.8±0.9	5.3±0.6	**4.8±0.4**
	48	9.1±1.1	8.6±1.1	**6.4±0.8**	**6.5±0.8**
	72	11.2±1.8	**9.8±1.3**	**7.6±0.9**	**7.7±0.7**